Double Loop Electrochemical Potentiokinetic Reactivation Test Optimization in Checking of Duplex Stainless Steel Intergranular Corrosion Susceptibility

T. AMADOU, C. BRAHAM, and H. SIDHOM

The double loop electrochemical potentiokinetic reactivation (DL-EPR) test using an electrolyte of 33 pct H_2SO_4 solution with 0.3 pct HCl, at room temperature and at a potential scan rate dE/dt of about 2.5 mV/s, was chosen to evaluate the sensitization of austeno-ferritic duplex stainless steels (DSS). Reproducible and optimal test responses and high test selectivity in detecting intergranular corrosion (IGC) susceptibility were verified for four DSS differing in their method of fabrication (cast or wrought) and their ferrite phase content (44 to 57 pct). The test was successfully used to analyze the interactions between precipitation, chromium depletion, and IGC sensitization of the UNS S31250 steel, which was aged between 6 minutes and 120 hours at temperatures varying from 500 °C to 900 °C. The eutectoid decomposition of the ferrite, at different aging temperatures, was investigated using various techniques. The chromium depletion was analyzed qualitatively by X-ray mapping in a scanning transmission electronic microscope (STEM) and quantitatively by analytical calculation based on the chromium diffusion in the ferrite. It was shown that the chromium content in the ferrite can decrease from 30 to 7.5 pct by weight during aging before total decomposition occurs. The interactions between precipitation and IGC sensitization during DSS aging were clearly shown by superimposing the time-temperature-start of precipitation (TTP) and time-temperature-sensitization (TTS) diagrams obtained from the DL-EPR tests performed for various levels of sensitization.

I. INTRODUCTION

AUSTENO-FERRITIC duplex stainless steels (DSS) are well known for their high resistance to all kinds of localized corrosion.[1–4] They are particularly resistant to the selective dissolution of chromium-depleted zones resulting from the precipitation of chromium carbides and intermetallic phases. This precipitation, sometimes inevitable, occurs when manufacturing conditions heat these stainless steels to temperatures ranging from 400 °C to 1050 °C.[5,6,7]

During reception inspection of finished stainless steel products, standard test types such as Strauss, *et al*.[8–11] are typically used to evaluate the intergranular corrosion (IGC) susceptibility. These tests are difficult to perform *in situ* and the interpretation of the results, especially in the case of a very thin precipitation, is very difficult. These tests require a significant quantity of material for testing, which is often detrimental to the service life of structures, and can affect the integrity of the pieces during the reception inspection.

Because of the need to insure nondestructive examinations, an electrochemical potentiokinetic reactivation (EPR) test was developed mainly to assess cast products.[12] Numerous studies[4,13–22] have contributed to the development of this technique over the years. The most common of the many variations of this technique used today is the double loop electrochemical potentiokinetic reactivation (DL-EPR) method,[14–17,23–25] which has the advantage of having only a weak dependence on surface texture.[22,23,24] Today, DL-EPR tests can be performed *in situ* using portable cell devices.[19] The DL-EPR test is very suitable for reception inspections of finished pieces and assembled devices.[20]

It has been demonstrated in numerous cases of stainless steel (SS) or nickel alloys[4,12–26] that the high sensitivity of this technique to the electrolyte composition and to operating conditions does not affect its reliability. Nevertheless, to detect the effect of very fine precipitations using the DL-EPR test, an appropriate electrolyte composition and temperature and appropriate conditions for potential limits and scan rates are required for each alloy.[4,19,22,26] The summary of technical literature related to austeno-ferritic DSS shows that the electrolyte often consists of sulfuric acid (H_2SO_4) solution with the addition of NaCl or KSCN as depassivators (Table I). However, hydrochloric acid (HCl) is used as the depassivator in the case of DL-EPR tests for super austenitic SS.[19] The potential scan rate remains between 0.5 and 5 mV/s and the chosen temperature is often the room temperature or close to 30 °C.[4,21,25,27–29]

The first objective of the present study is to determine the optimum conditions leading to a quantitative evaluation of the IGC susceptibility of four austeno-ferritic DSS using the DL-EPR test. Particular attention will be given to the IGC sensitivity detection threshold when the performance comparison with various existent conditions[4,21,25,27–29] will be carried out. The optimized test conditions determined in this first part will be applied to determine the interactions between precipitation, chromium depletion, and IGC sensitization of the aged UNS S31250 steel.

T. AMADOU, Lecturer, and H. SIDHOM, Professor, are with the Laboratoire de Mecanique, Matériaux et Procédés, 1008 Tunis, Tunisia. C. BRAHAM, Senior Lecturer, is with the Laboratoire de Microstructure et Mécanique des Matériaux, F75013 Paris, France. Contact e-mail: braham@paris.ensam.fr

Manuscript submitted October 23, 2001.

Table I. Operating Conditions to Evaluate DSS IGC Sensitization by DL-EPR Test

Steel Type	Heat Treatment	Operating Conditions of DL-EPR Test of DSS: Temperature of Electrolyte (°C)	Composition of the Electrolyte	Potential Scan Boundaries (mV/SCE)	Potential Scan Rate (mV/s)	Evaluation Criterion of IGC Sensitization: I_r/I_a	Etching Structure	References
X2CrNi Mo 22-5	solution annealing (1100 °C-20 mn)	30	H_2SO_4 2M + NaCl 0.5M + KSCN 0.01M	−400 ↔ +200	1.67	0.01×10^{-2}	step	4
						0.81×10^{-2}	dual	
	675 °C-1 h					8.14×10^{-2}	ditch	
	675 °C-2 h					24.7×10^{-2}	ditch	
	675 °C-10 h							
UNS S31803	solution annealing (1100 °C-20 mn)	30	H_2SO_4 2M + NaCl 0.5M + KSCN 0.01M	$E_{Cor.}$ ↔ +200	1.67	0	step	21
					1	0.03×10^{-2}	dual	
						$0.05 \times 10^{-}$	dual	
X3CrNi Mo22-5-3	675 °C-1 h					5×10^{-2}	ditch	
	675 °C-2 h					9×10^{-2}	ditch	
	675 °C-5 h					30×10^{-2}	ditch	
	675 °C-10 h							
	900 °C-4 h							
	solution annealing aged state			−600 ↔ +200		0.8×10^{-2}	—	25
						1.1×10^{-2}		
AISI 308L 22 pct δ	solution annealing (deposited metal)	30	H_2SO_4 0.5M + NaCl 0.01M	−500 ↔ +300	—	0.71×10^{-2}	—	27
	700 °C-1 h					3.3×10^{-2}		
						2.5×10^{-2}		
	700 °C-10 h					1.5×10^{-2}		
						1.04×10^{-2}		
	700 °C-100 h					1.9×10^{-2}		
						1.3×10^{-2}		
CF-8 cast	solution annealing	30	H_2SO_4 0.5M + KSCN 0.02M	$E_{Cor.}$ ↔ +450	0.83	0.01×10^{-2}	—	28
	800 °C-1 h					0.2×10^{-2}		
	700 °C-0.5 h					0.44×10^{-2}		
	600 °C-15 h					3.96×10^{-2}		
UNS S32550	—	30	H_2SO_4 0.5M + KSCN 0.02M	$E_{Cor.}$ ↔ +450	1.67	—	—	29

Step: step between the grains, no sensitization.
Dual: ditches at grain boundaries, but no grain completely encircled.
Ditch: one or more grains completely surrounded by ditches.

II. MATERIALS AND TESTS

A. *Materials and Heat Treatments*

Four austeno-ferritic DSS materials were studied. The main differences between them concern their methods of fabrication, chemical compositions, and ferrite-phase contents. All alloy elements and ferrite-phase contents are shown in Table II. The studied steels were subjected to a solution annealing consisting of air cooling after holding for 2 hours at 1170 °C, followed or not by a sensitization treatment of 10 hours at 750 °C. Another aging treatment corresponding to a low sensitization, 1 hour at 600 °C, was applied to the steel A (UNS S31250) to verify the sensitivity of the test in detecting the effect of a low chromium depletion.

To determine the time-temperature-start of precipitation (TTP) diagram and analyze the interactions between precipitations and IGC sensitization in the case of the same steel A, other aging treatments were performed at temperatures ranging from 500 °C to 900 °C during time periods ranging from 6 minutes to 120 hours.

B. *Tests and Methods*

1. *Analyses of aged structures*

The structure of aged and annealed steels was analyzed by optical microscopy (OM) and scanning electronic microscopy (SEM). Precipitated phases were identified using transmission electronic microscopy (TEM). Their chemical compositions were determined by X-ray microanalysis in the scanning transmission electronic microscope (STEM), using extractive replica. The ferrite decomposition due to aging treatments was quantified by the magnetic method and its chromium depletion was evaluated qualitatively by X-ray mapping using K_α Cr radiation, in the STEM. The quantitative evaluation

Table II. Chemical Composition (Weight Percent) and Ferrite Content (Volume Percent) of DSS

Reference in This Study	Standard Designation of Steels	Elaboration Mode	C	Cr	Ni	Mo	Cu	Mn	N	Si	Fe	Ferrite Content
A	UNS S31250	cast	0.068	25.56	6.69	2.52	2.32	0.59	0.137	0.7	bal	44.25
B	UNS S31260		0.07	22.63	8.38	2.57	1.44	0.82	0.089	0.64	bal	46.14
C	UNS S31803		0.03	21.79	5.34	2.88	0.31	1.48	—	0.45	—	50
D	UNS S32404	wrought	0.025	21.67	7.03	2.65	1.0	0.41	0.032	0.85	bal	57.2

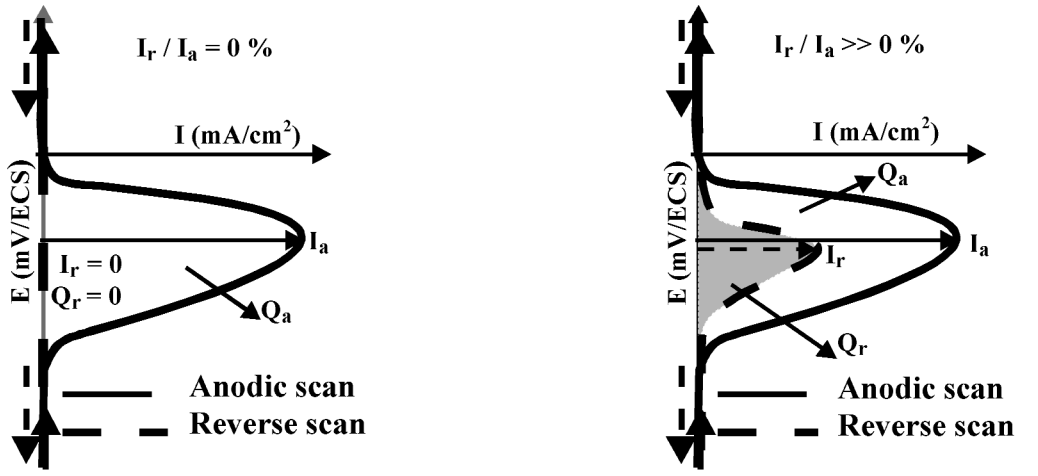

a) Non sensitized material

b) Sensitized material

I_a = activation current density (anodic)

I_r = reactivation current density (reverse)

Q_a = activation charge density (anodic)

Q_r = reactivation charge density (reverse)

Sensitisation criterion [19].

	Solution annealed material	Aged material
I_r / I_a (%)	< 1	≥ 1
Q_r / Q_a (%)	< 1	≥ 1

Fig. 1—Principle of DL-EPR technique and IGC sensitization criterion: (a) nonsensitized material and (b) sensitized material.

of this depletion was performed using an analytical model based on the chromium-diffusion kinetic in the ferrite.

2. *Double Loop Electrochemical Potentiokinetic Reactivation Tests*

The sensitivity of aged DSS to IGC was evaluated using the DL-EPR test, which consists of a potentiokinetic scanning in a suitable electrolyte, from an active to a passive domain (activation or anodic scan), followed by a return to the initial potential (reverse or reactivation scan). The ratio of reactivation and anodic current densities (I_r/I_a pct) and the ratio of reactivation and anodic current charges (Q_r/Q_a pct) permit the evaluation of the degree of sensitization (Figure 1).

The DL-EPR test efficiency is measured by means of a response test, which must be characterized by weak values of the current density ratio ($I_r/I_a < 1$ pct) and the charge ratio ($Q_r/Q_a < 1$ pct) for nonsensitized materials, and relatively high ratio values ($I_r/I_a \geq 1$ pct and $Q_r/Q_a \geq 1$ pct) for high-sensitized materials. For the latter materials, anodic and reactivation current densities must also be high enough to lead to peaks clearly perceptible by the operator. In addition, the test selectivity must be confirmed by the existence of only one reactivation peak related to intercrystalline chromium depletion. The test accuracy is evaluated by its aptitude to detect the effect of low amounts of chromium depletion corresponding to the fine precipitations of carbides or high-chromium intermetallic phases at α/γ interfaces.

Obtaining the best test result requires control of the test operating conditions (depassivator concentration, electrolyte temperature, boundaries, and potential scan rate).

III. RESULTS

A. *Structure of Aged Steels*

The structures of annealed steels do not reveal any visible precipitation (Figure 2). The structures corresponding to the sensitization treatment (10 hours at 750 °C) are marked by an eutectoid decomposition of the ferrite phase, which

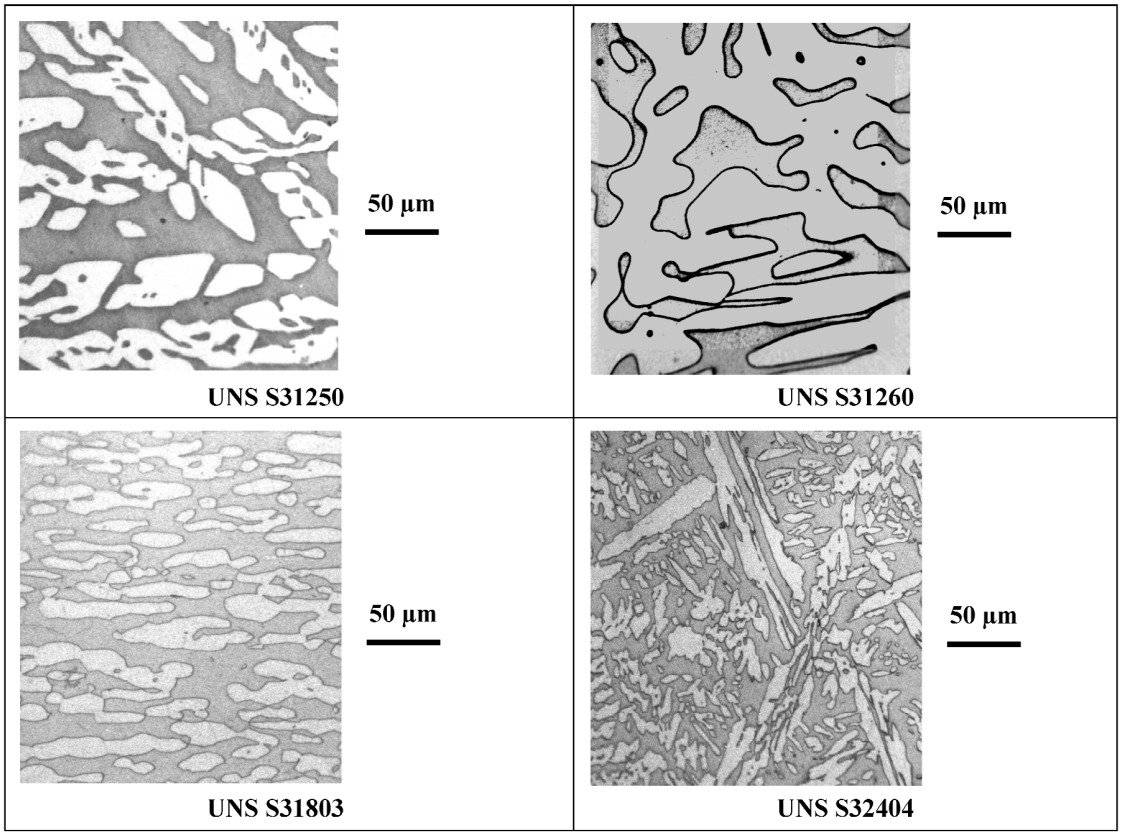

Fig. 2—Structure of solution-annealed materials (1170 °C-2 h/air).

is transformed partially or totally into regenerated austenite (γ_r), chromium carbides, and intermetallic phases (Figures 3(a) through (d)). The attained state of the aged ferrite decomposition depends on the chemical composition of the steel. The low-sensitized treatment (1 hour at 600 °C) applied to steel A produces a structure with a low discontinuous precipitation of carbides at α/γ interfaces and at grain boundaries α/α, describing a substructure clearly visible as ferrite isles (Figures 3(e) and (f)).

B. *Influence of the Electrolyte Type*

The electrolyte consisted of a 33 pct sulfuric acid (H_2SO_4) solution with a controlled addition of hydrochloric acid (HCl) as a depassivator agent. The results, corresponding to tests performed at temperatures under 20 °C and with a potential scanning rate of 2.5 mV/s, show that the best DL-EPR response is obtained with a HCl electrolyte concentration of about 0.3 pct (Figure 4).

The solution-annealed steels (nonsensitized) retain the ratios $I_r/I_a < 1$ pct (Figure 4(a)). The significant increase in the current density ratio ($I_r/I_a > 1$ pct), related to the solution-annealed wrought steel UNS S32404 (steel D) with the electrolyte HCl concentration, results certainly from the lower potential scanning rate ($dE/dt = 2.5$ mV/s) compared with the recommended rate (3 times higher) for this type of product.[19] The optimal ratios $I_r/I_a > 70$ pct and $Q_r/Q_a > 50$ pct (Figure 4(b)) correspond to the markedly sensitized steels. The activation and reactivation current densities are high enough to give clearly perceptible peaks ($I_r > 15$ mA/cm^2) (Figure 5(a)). The low-sensitization treatment (1 hour at 600 °C) of steel A leads, in these conditions, to a ratio ($I_r/I_a = 2.1$ pct), very much lower than the ratio found for the high-sensitization treatment (10 hours at 750 °C) of the same steel ($I_r/I_a = 90$ pct). The test selectivity is insured by the presence of a unique reactivation peak at a potential of −115 mV/SCE, related to IGC. Higher HCl concentrations (>0.3 pct) do not substantially modify the I_r/I_a ratio, but they do weaken the DL-EPR test selectivity by favoring the appearance of a second reactivation peak. It appears in the case of cast-sensitized steel, at a potential of −290 mV/SCE. The latter has a lower current density and so-called "uniform corrosion peak" and is followed by pitting corrosion in the austenite γ (Figure 5(b)).

C. *Influence of the Potential Scan Rate*

The DL-EPR tests in a 33 pct sulfuric acid solution were conducted with potential scan rates varying from 0.5 to 5 mV/s and under constant conditions of hydrochloric acid (HCl) addition (0.3 pct) at 20 °C. The results reveal an optimal test response for rates equal to or higher than 2.5 mV/s (Figure 6). The different solution-annealed steels tested show a ratio $I_r/I_a < 1$ pct (Figure 6(a)). The markedly sensitized steels show an optimal ratio ($I_r/I_a > 70$ pct and $Q_r/Q_a > 50$ pct) at a scanning rate of 2.5 mV/s higher than in the case of the weakly sensitized (1 hour at 600 °C) steel type UNS S31250 ($I_r/I_a = 2.1$ pct) (Figure 6(b)). Anodic and reactivation current

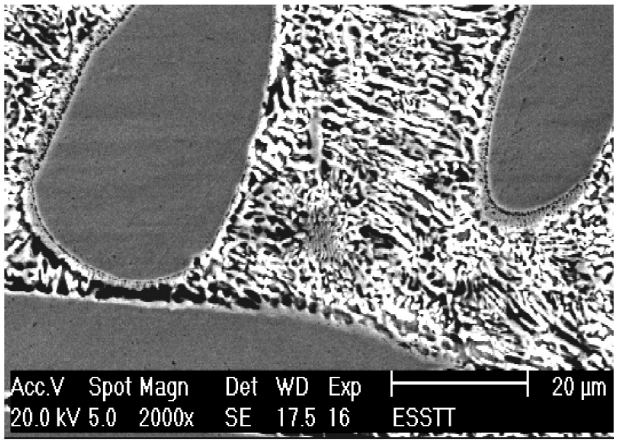

a) UNS S31250 (750°C – 10h / Air)

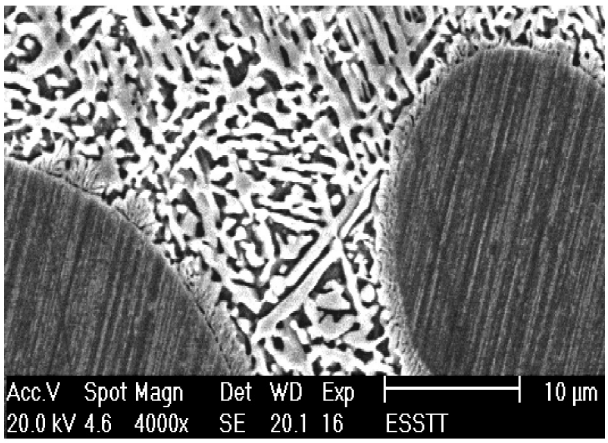

b) UNS S31260 (750°C – 10h / Air)

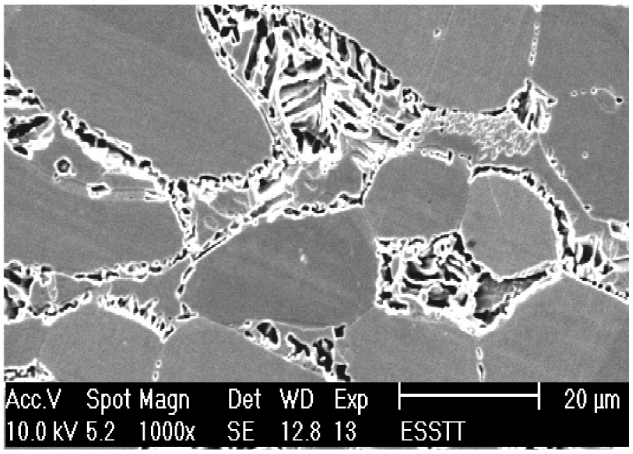

c) UNS S31803 (750°C – 10h / Air)

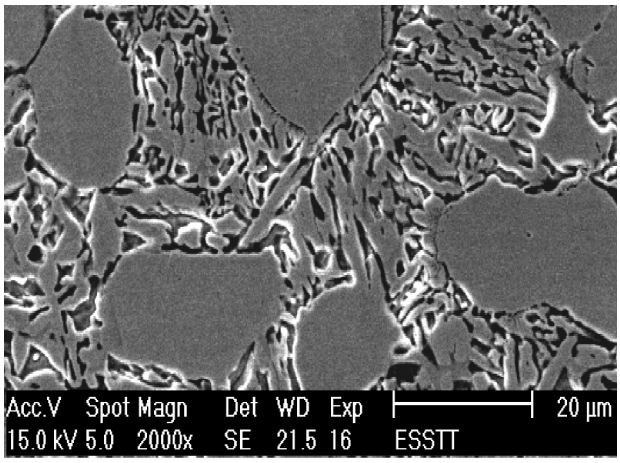

d) UNS S32404 (750°C – 10h / Air)

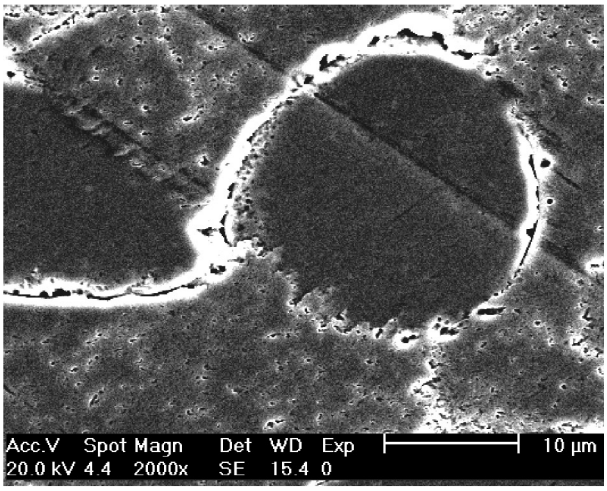

e) UNS S31250 (600°C - 1h / Air)

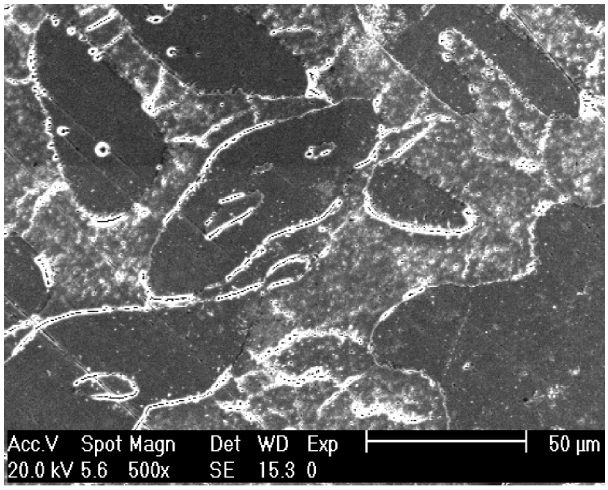

f) UNS S31250 (600°C - 1h / Air)

Fig. 3—Structure of sensitized materials: (a) UNS S31250 (750 °C-10 h/air), (b) UNS S31260 (750 °C-10 h/air), (c) UNS S31803 (750 °C-10 h/air), (d) UNS S32404 (750 °C-10 h/air), (e) UNS S31250 (600 °C-1 h/air), and (f) UNS S31250 (600 °C-1 h/air)

densities are high enough to yield a clearly perceptible reactivation peak (at −115 mV/SCE) corresponding to IGC (Figure 7(a)). The test remains selective, with only one corresponding peak of reactivation.

At lower potential scanning rates ($dE/dt < 2.5$ mV/s), the test selectivity markedly decrease: the ratio of I_r/I_a becomes higher than 1 pct for solution-annealed materials and a second peak relative to uniform corrosion appears at a potential of

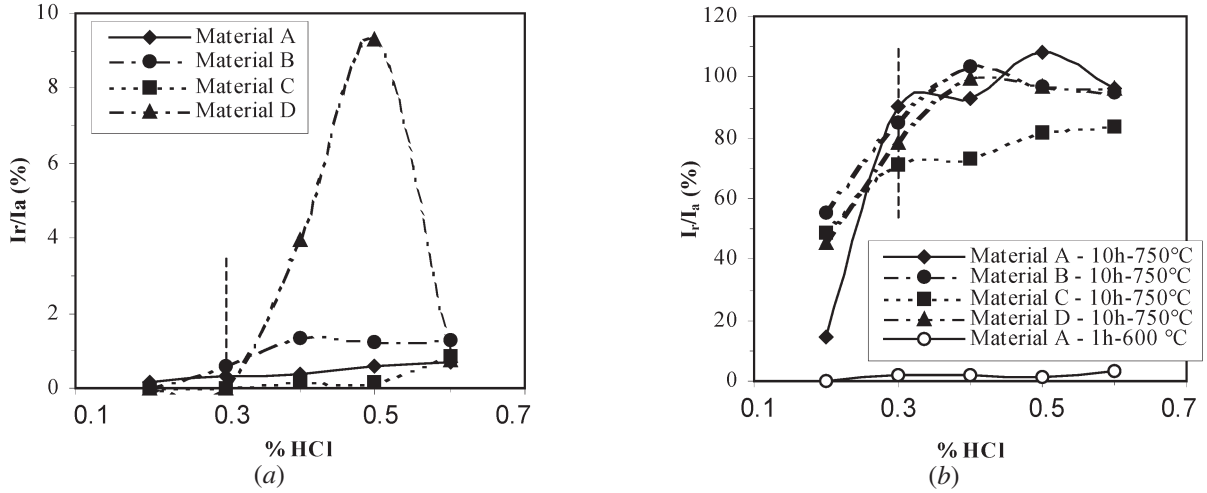

Fig. 4—Influence of hydrochloric acid (HCl) concentration on the DL-EPR test response in the case of DSS tested in a solution containing 33 pct H_2SO_4 + *x* pct HCl at *dE/dt* = 2.5 mV/s and *T* = 20 °C: (*a*) solution-annealed materials (1170 °C-2 h/air) and (*b*) sensitized materials (750 °C-10 h/air and 600 °C-1 h/air).

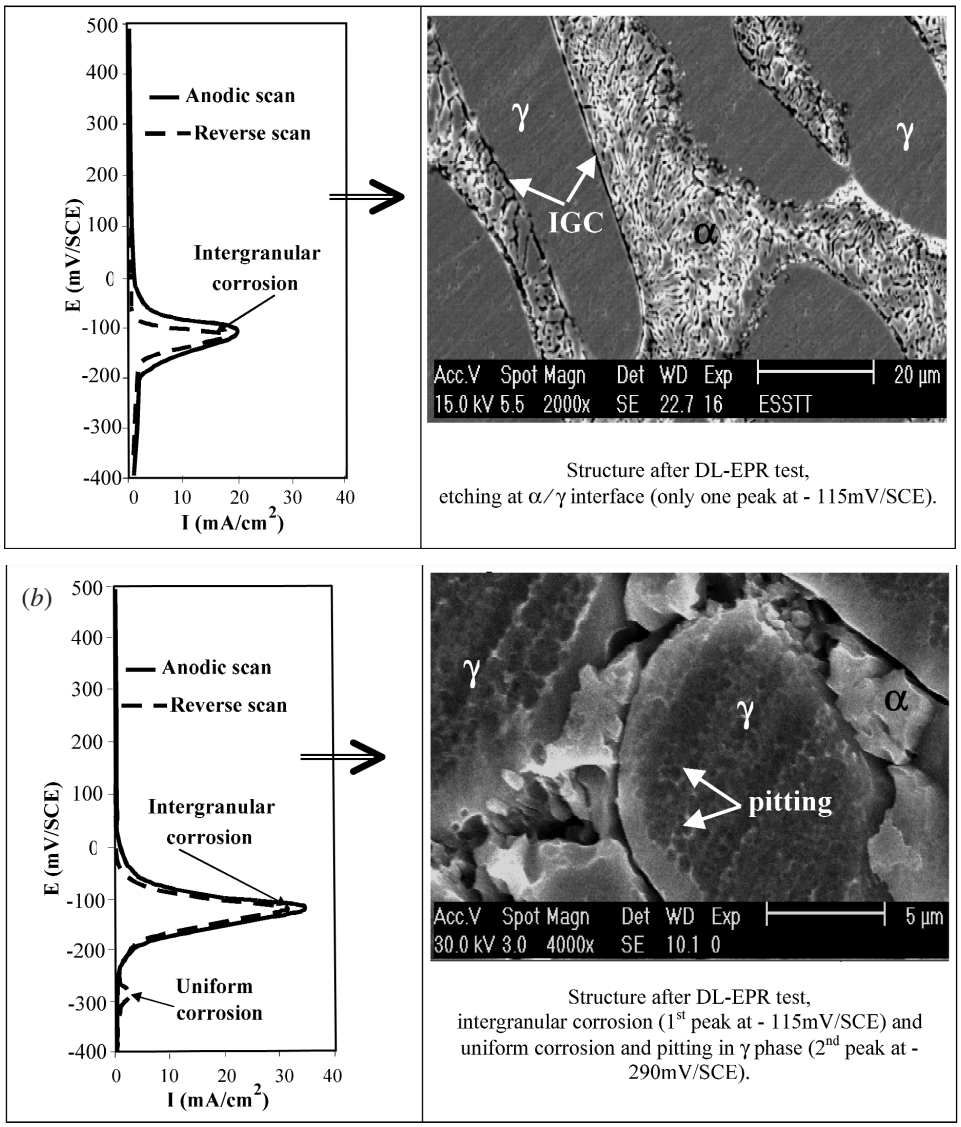

Fig. 5—Influence of HCl concentration on the DL-EPR test selectivity, steel UNS S31250 (750 °C-10 h/air) at *dE/dt* = 2.5mV/s and 20 °C: (*a*) 33 pct H_2SO_4 + 0.3 pct HCl and (*b*) 33 pct H_2SO_4 + 0.4 pct HCl.

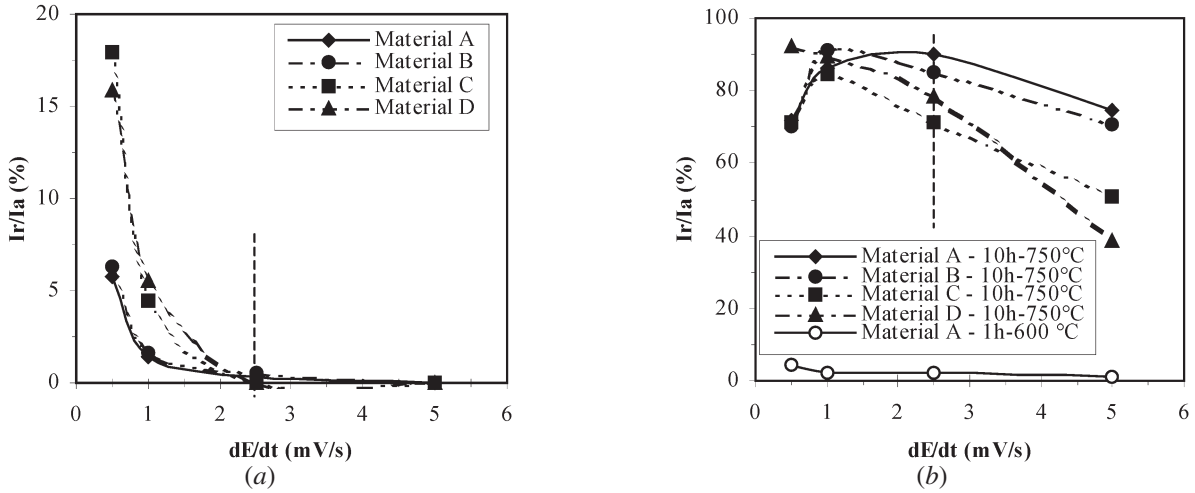

Fig. 6—Influence of potential scan rate on the DL-EPR test response, DSS tested in an electrolyte containing 33 pct H_2SO_4 + 0.3 pct HCl, at 20 °C: (*a*) solution-annealed states (1170 °C-2 h/air) and (*b*) sensitized materials (750 °C-10 h/air and 600 °C-1 h/air).

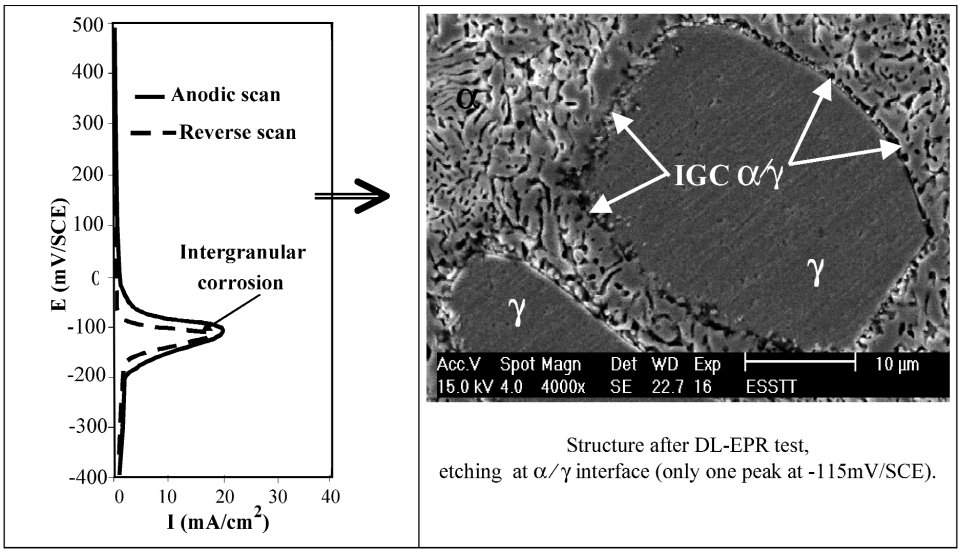

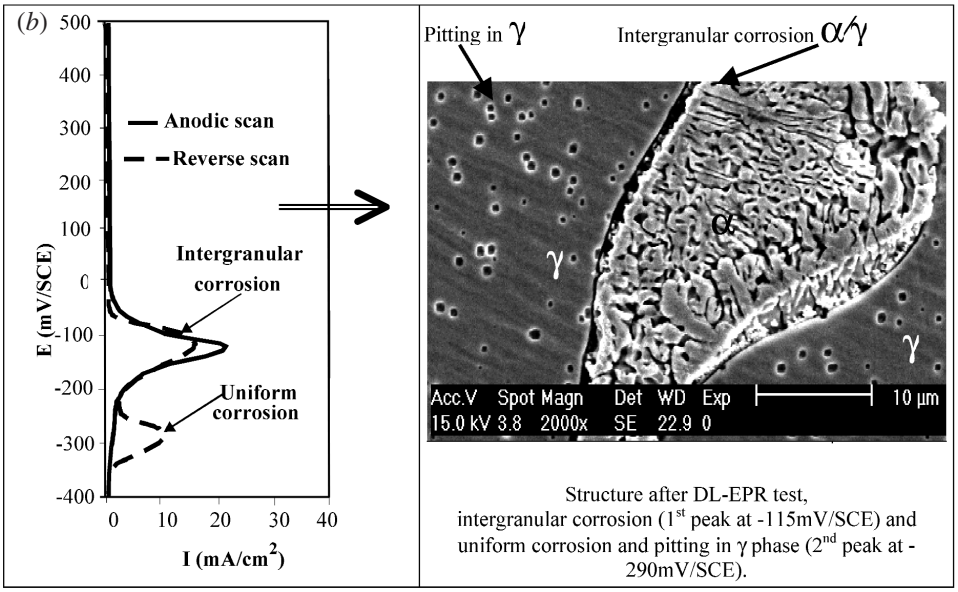

Fig. 7—Influence of potential scan rate on the DL-EPR test selectivity, DSS type UNS S31250 (750 °C-10 h/air) with 33 pct H_2SO_4 + 0.3 pct HCl, at 20 °C: (*a*) dE/dt = 2.5 mV/s and (*b*) dE/dt = 0.5 mV/s.

−290 mV/SCE, for sensitized materials, with a high density of pits localized in the austenitic phase (Figure 7(b)).

D. *Influence of the Temperature*

The DL-EPR tests were carried out at different temperatures from 20 °C to 35 °C, with fixed conditions of the potential scanning rate (2.5 mV/s) and electrolyte concentrations (33 pct H_2SO_4 + 0.3 pct HCl). The optimal DL-EPR test response is obtained with the electrolyte at 20 °C (Figure 8). A weak current ratio ($I_r/I_a < 1$ pct) is observed with all solution-annealed steels (Figure 8(a)). Markedly sensitized materials give very high ratios ($I_r/I_a > 70$ pct and $Q_r/Q_a > 50$ pct), compared to weakly sensitized materials ($I_r/I_a = 2.1$ pct), (Figure 8(b)). The activation and reactivation current densities are high enough to lead to clearly perceptible reactivation peaks (at −115 mV/SCE) corresponding to IGC (Figure 9(a)). The test still remains selective, with only one reactivation peak corresponding to IGC (at −115 mV/SCE).

At higher temperatures, the ratio I_r/I_a obtained with sensitized materials is higher than that obtained at 20 °C, but the related sensitivity is weaker because of the appearance of the second reactivation peak at −290 mV/SCE, with a lower current density, corresponding to uniform corrosion, and followed by the apparition of pits into the austenite (γ) (Figure 9 (b)).

E. *Optimal Operating Conditions and Reproducibility of Tests*

The optimal operating conditions of the IGC evaluation test established in this study are compared to other in Table III. These conditions are more selective and efficient. They offer the best ratio I_r/I_a for the high-sensitization treatment with the best sensitivity in the case of the weak-sensitization treatment (1 hour at 600 °C). The reproducibility of the DL-EPR test has been verified through tests performed with UNS S31250 DSS specimens sensitized at 800 °C over 10 hours, in the optimized conditions of the test, but repeated after two periods (24 and 8000 hours). The results, reported in Table IV, show only a very low variation of the ratio I_r/I_a (in percent) characterizing the sensitization degree of the same aged material, with the age of the electrolyte (33 pct H_2SO_4 + 0.3 pct HCl).

F. *Interactions between Precipitation, Chromium Depletion, and IGC*

The optimized test conditions determined in this study will be applied to determine the interactions between precipitation, chromium depletion, and IGC sensitization of the UNS S31250 steel aged in time periods ranging from 6 minutes to 120 hours at temperatures varying from 500 °C to 900 °C.

1. *Precipitation*

The evolution of the structure of the annealed UNS S31250 steel during isothermal holding between 500 °C and 900 °C is controlled by the precipitation into the ferrite phase (magnetic), which decomposed into regenerated austenite, chromium carbides, and intermetallic phases (paramagnetic). This decomposition is very fast near 800 °C, and, at this temperature, it is quasi-total after 10 hours (Figure 10). The precipitation sequence is characterized by the appearance at the α/γ interfaces, at temperatures from 500 °C to 650 °C, of a thin film of Fe-Cr-Mo intermetallic phase, called phase I in previous studies.[30,31] This phase is characterized in electronic diffraction by a crystalline structure like an icosaedric phase (Figure 11). For longer holding at these relatively low temperatures, a nucleation of $M_{23}C_6$ carbides occurs at the α/γ interfaces (Figure 12) and these grow in the place of the ferrite, which decomposes totally with respect to the reaction: $\alpha \rightarrow I + M_{23}C_6 + \eta + \gamma_r$. At higher temperatures, the ferrite decomposition occurs more in line with the following eutectoid reaction: $\alpha \rightarrow M_{23}C_6 + \sigma + \eta\ \gamma_r + \chi + R$ with a preponderance of σ phase (Figure 13). The results of the metallographic analyses of aged structures are presented in Table V (columns G and H). The chemical compositions of the main created phases, determined by X-ray microanalysis of extractive replica using STEM, are reported in Table VI.

2. *Chromium depletion*

Phase I, and particularly the carbides, precipitate at low temperatures, and the σ phase precipitates at higher temperatures; these are rich in chromium, which is provided

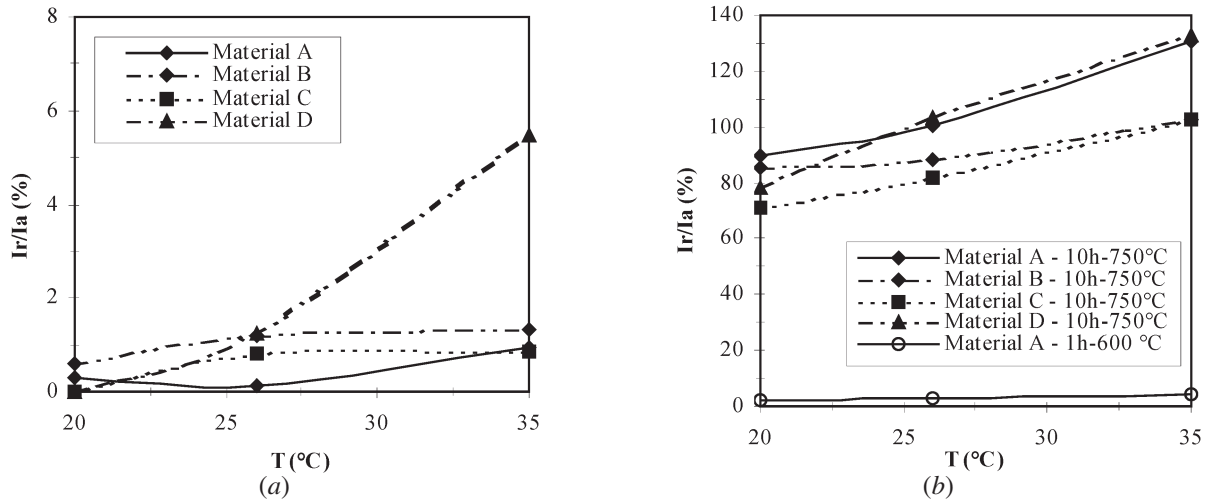

Fig. 8—Influence of the temperature on the DL-EPR test response, DSS tested in an electrolyte containing 33 pct H_2SO_4 + 0.3 pct HCl: (*a*) solution-annealed materials (1170 °C-2 h/air) and (*b*) sensitized materials (750 °C-10 h/air and 600 °C-1 h/air).

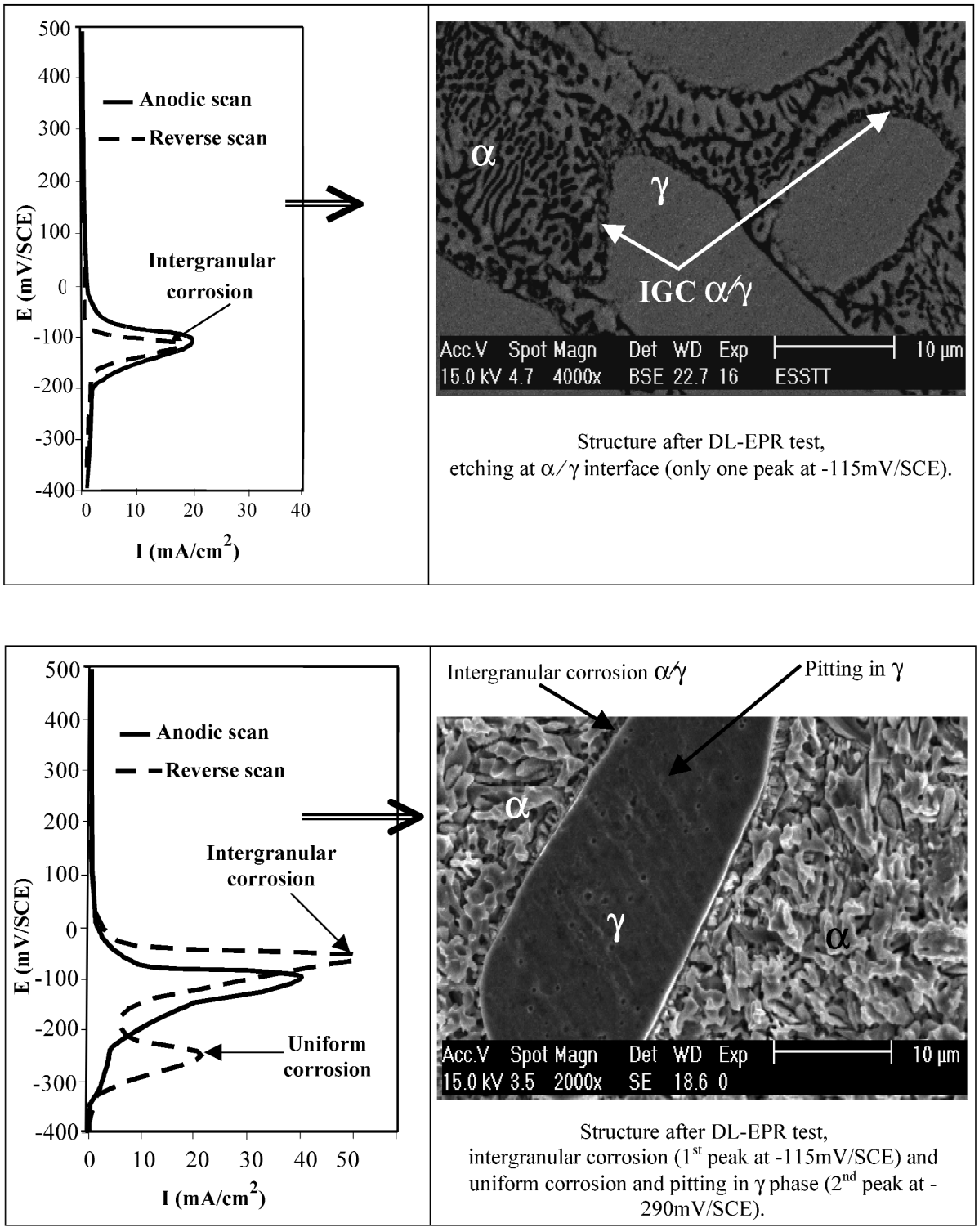

Fig. 9—Influence of the temperature on the DL-EPR test selectivity, steel A (750 °C-10 h) tested in an electrolyte containing 33 pct H_2SO_4 + 0.3 pct HCl: (*a*) $T = 20$ °C and (*b*) $T = 35$ °C.

Table III. Influence of the Depassivator Type on the DL-EPR Test Responses, Case of Steel A (UNS S31250)

Heat Treatment	Qualitative Evaluation of IGC Sensitization Using Optical Metallography	Qualitative Evaluation of IGC Sensitization Using the DL EPR Test	Conditions of This Study: 33 Pct H_2SO_4 + 0.3 Pct HCl; T = 20 °C; dE/dt = 2.5 mV/s	Conditions of References 28 and 29: H_2SO_4 0.5M + KSCN 0.02M; T = 30 °C; dE/dt = 0.83 mV/s	Conditions of References 4, 21, and 25: H_2SO_4 2M + KSCN 0.01M + NaCl 0.5M; T = 30 °C; dE/dt = 1.67 mV/s
Solution annealing 1170 °C-2 h	nonsensitized step	I_r (mA/cm^2)	0.03	0	0.07
		I_r/I_a (pct)	0.3	0	0.89
Aging 600 °C-1 h	weakly sensitized dual	I_r (mA/cm^2)	0.20	0.0004	0.16
		I_r/I_a (pct)	2.10	0.08	1.81
Aging 750 °C-10 h	markedly sensitized ditch	I_r (mA/cm^2)	17.8	0.016	12.6
		I_r/I_a (pct)	90.08	0.12	38

Table IV. DL-EPR Test Reproducibility, Case of Steel A (UNS S31250) Tested in 33 Pct H_2SO_4 + 0.3 Pct HCl Solution

Heat Treatment	Sensitivity of DL EPR Test	Test 1	Test 2: after 24 h	Test 3: after 8000 h
Aging 800 °C-10 h air cooling	I_a (mA/cm^2)	38.96	37.5	40.2
	I_r (mA/cm^2)	33.93	32.94	35
	I_r/I_a (pct)	87.9	87.84	87.06
	Q_r/Q_a (pct)	—	65.55	—

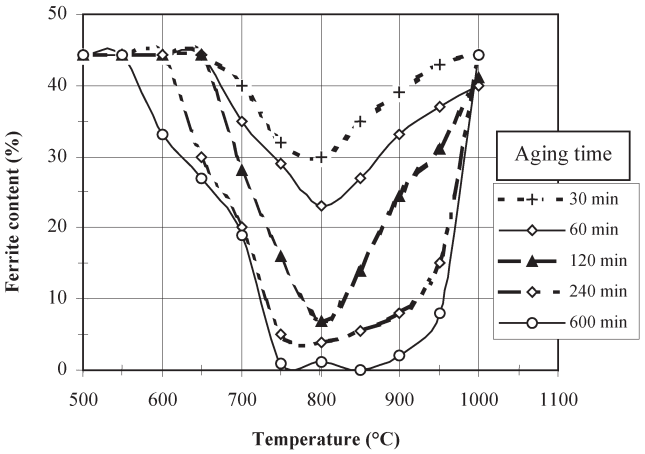

Fig. 10—Evolution of the ferrite content with aging time. Isothermal holding at the temperature range from 600 °C to 1000 °C, DSS type UNS S31250.

of Sahlaoui *et al.*[32] Chromium profiles around grain boundaries can be predicted by the model equation:

$$x_{Cr}(x,t) = x^i_{Cr}(t) + (x^0_{Cr} - x^i_{Cr}(t)) \cdot erf\left(\frac{x}{2\sqrt{Dt}}\right) \quad [1]$$

where x^0_{Cr} is the chromium initial concentration of the matrix and $x^i_{Cr}(t)$ is the chromium concentration at matrix-carbide interfaces obtained at a chromium depletion state, with the equation:

$$x^i_{Cr}(t) = x^0_{Cr} \exp\left(-k\frac{t}{\tau}\right) \quad [2]$$

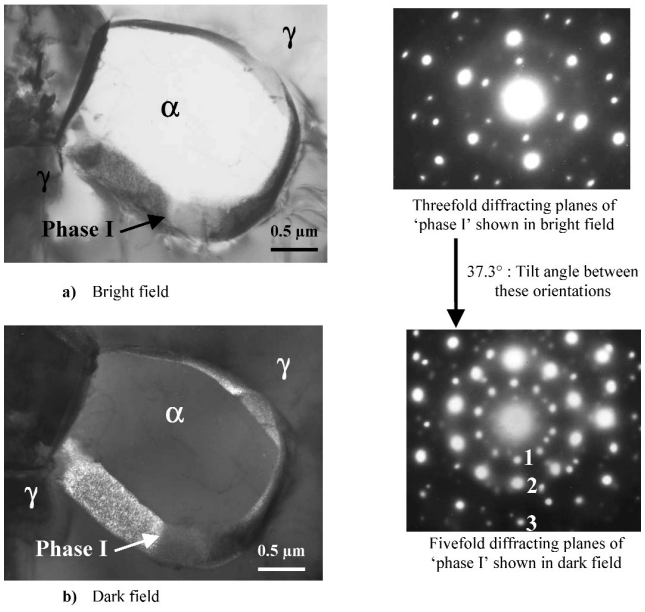

Fig. 11—Precipitation of intermetallic phase type I after aging for 10 h at 550 °C, DSS type UNS S31250: (*a*) bright field and (*b*) dark field.

where

τ = 4 h,
$k_{Ferrite}$ = 1.695, and
$k_{Austenite}$ = 0.088.

Profiles obtained by these equations, related to isotherm holding at 600 °C, show a significant chromium depletion of the ferritic phase compared to the depletion of the austenitic phase (Figure 15). This is imputed to the chromium diffusion kinetic, which is about 100 times slower in the austenitic phase (γ) than in the ferritic phase (α). The minimum chromium content of the ferrite, calculated using the model, reached after 3 hours at 600 °C, is about 7.5 wt pct. This agrees with experimental results obtained by X-ray microanalysis in the case of CF8M steel aged at 600 °C for 2000 hours[33] (Figure 16).

3. *IGC sensitization*

Using the optimal conditions determined in this study, DL-EPR testing was performed to evaluate qualitatively the degree of sensitization of UNS S31250 steel aged according

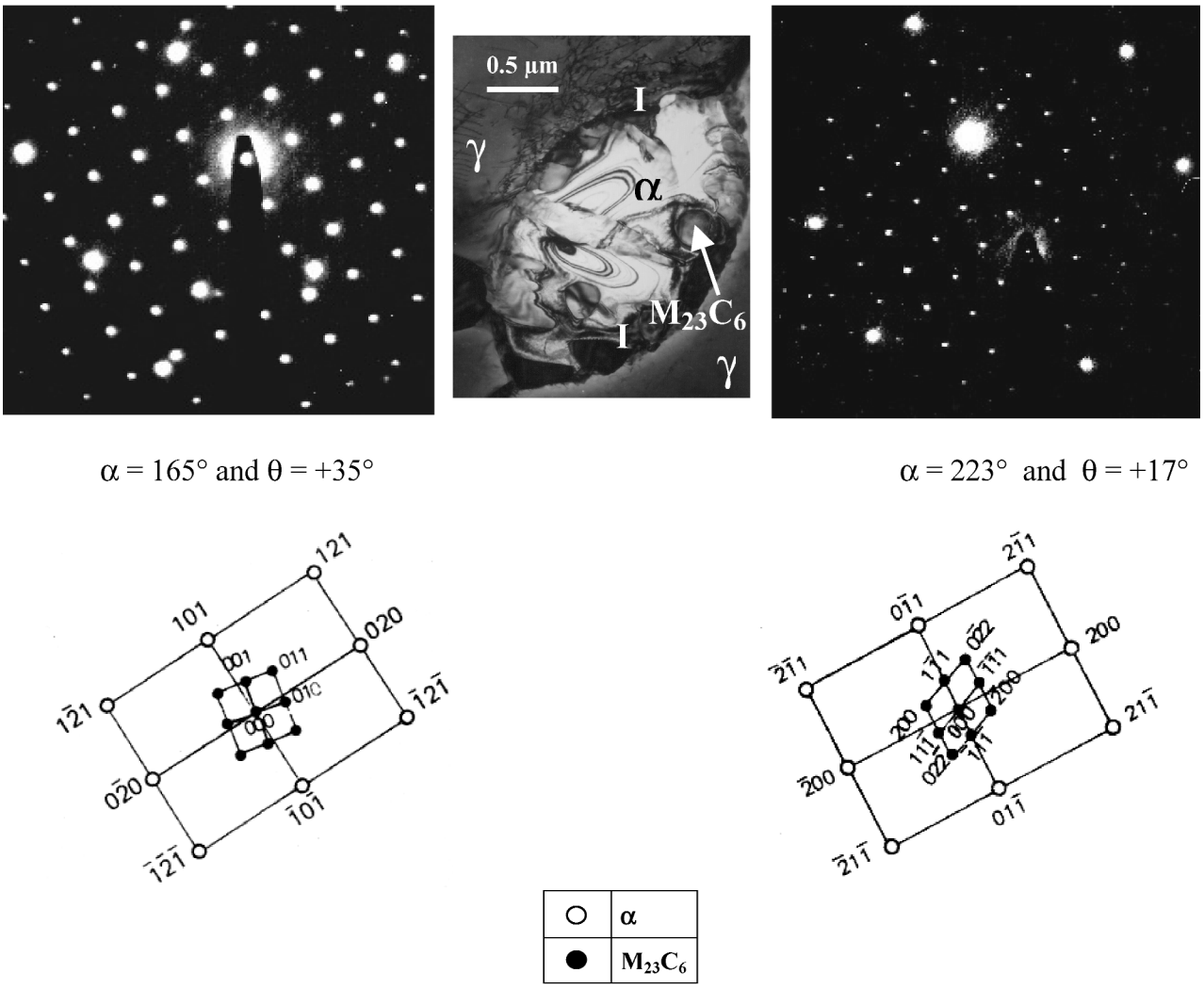

Fig. 12—Start of precipitation of $M_{23}C_6$ carbides after aging at 550 °C (100 h), UNS S31250 DSS.

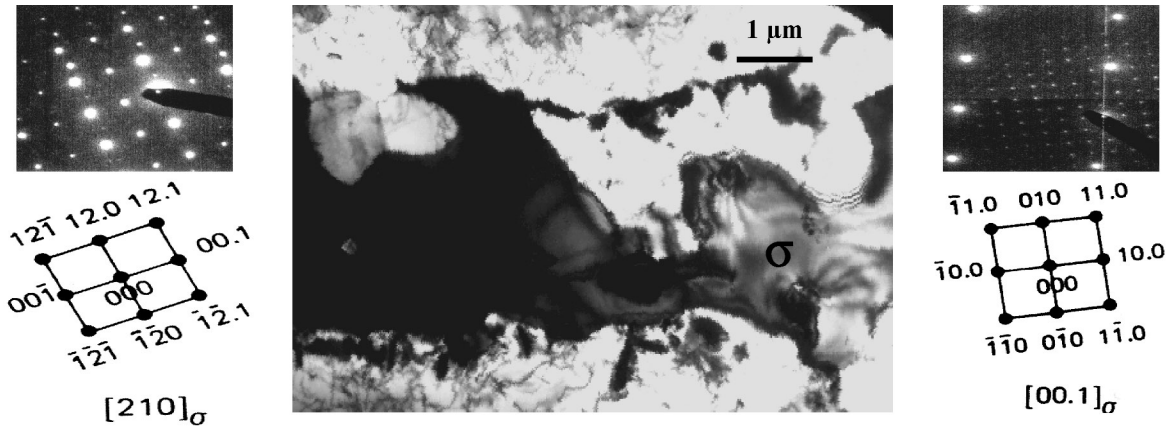

Fig. 13—Eutectoid decomposition of the ferrite at high temperature ($\alpha \rightarrow M_{23}C_6 + \gamma_r + \sigma + \chi + R$) after holding for 10 h at 800 °C.

to the conditions in Table V. This table also contains the ratios I_r/I_a (percent) and Q_r/Q_a (percent) (columns I and J). On the basis of these ratios, a time-temperature-sensitization (TTS) diagram was drawn and superimposed on the TTP diagram (Figure 17), in order to highlight the effect of the principal phases created on the IGC sensitization.

Table V. Results of DL-EPR Test and Etching Structures Related to Steel Type UNS S31250 with Varying Aging Conditions

E	F	G	H	I	J
		Microstructural Analyses		IGC Sensitization	
Temperature (°C)	Time (min)	Interfaces α/γ	Intra α	I_r/I_a (pct)	Q_r/Q_a (pct)
500	600	I	—	0	0
	6000	I	η	3.7	9.67
550	240	I	—	0	0
	600	I	—	3.90	6.80
	900	I	—	10.97	13.90
	1200	$I + M_{23}C_6$	—	16.61	17.25
600	30	I	—	0	0
	60	I	—	2.10	3.39
	120	I	—	3.68	7.22
	180	$I + M_{23}C_6$	η	18.10	27.21
	240	$I + M_{23}C_6$	η	19.36	35.19
	600	$I + M_{23}C_6$	η	27.63	20.23
	2880	$I + M_{23}C_6$	$\eta + \gamma_r$	39.34	26.66
	7200	$I + M_{23}C_6$	$\eta + \gamma_r$	52.62	46.76
650	10	I	—	0.91	0.54
	30	I	η	4.59	8.11
	60	$I + M_{23}C_6$	η	15.46	22.76
	120	$I + M_{23}C_6$	$\eta + \gamma_r$	21.28	29.35
	240	$I + M_{23}C_6$	$\eta + \gamma_r$	26.75	34.81
700	6	$M_{23}C_6$	—	8.21	14.52
	12	$M_{23}C_6$	$\eta + \gamma_r$	16.55	21.89
	30	$M_{23}C_6$	$\eta + \gamma_r$	27.10	28.46
	60	$M_{23}C_6$	$\eta + \gamma_r + M_{23}C_6$	35.20	31.37
	120	$M_{23}C_6$	$\eta + \gamma_r + M_{23}C_6 + \sigma$	58.43	37.20
	240	$M_{23}C_6$	$\eta + \gamma_r + \sigma + \chi + R$	52.83	52.15
	600	$M_{23}C_6$	$\eta + \gamma_r + \sigma + \chi + R$	40.26	40.86
750	6	$M_{23}C_6$	—	11.98	15.47
	12	$M_{23}C_6$	—	15.58	18.28
	30	$M_{23}C_6$	γ_r	23.23	19.59
	60	$M_{23}C_6$	$\eta + \gamma_r + \sigma + \chi + R$	42.36	26.47
	120	$M_{23}C_6$	$\eta + \gamma_r + \sigma + \chi + R$	63.33	50.54
	258	$M_{23}C_6$	$\eta + \gamma_r + \sigma + \chi + R$	79.73	61.35
	600	$M_{23}C_6$	$\eta + \gamma_r + \sigma + \chi + R$	90.08	59.76
800	6	$M_{23}C_6$	—	16.50	18.21
	15	$M_{23}C_6$	—	37.24	34.63
	60	$M_{23}C_6$	$\eta + \gamma_r + \sigma$	27.49	21.27
	120	$M_{23}C_6$	$\eta + \gamma_r + \sigma + \chi + R$	51.96	37.22
	240	$M_{23}C_6$	$\eta + \gamma_r + \sigma + \chi + R$	79.90	54.20
	600	$M_{23}C_6$	$\eta + \gamma_r + \sigma + \chi + R$	87.84	65.55
850	6	$M_{23}C_6$	$\eta + \gamma_r + \sigma + \chi + R$	3.68	7.22
	60	$M_{23}C_6$	$\eta + \gamma_r + \chi + R$	31.18	22.96
	120	$M_{23}C_6$	$\eta + \gamma_r + \sigma + \chi + R$	24.26	19.16
	240	$M_{23}C_6$	$\eta + \gamma_r + \sigma + \chi + R$	45.28	27.88
	600	$M_{23}C_6$	$\eta + \gamma_r + \sigma + \chi + R$	57.62	33.20
900	12	$M_{23}C_6$	—	0.59	0.86
	18	$M_{23}C_6$	—	0.55	0.30
	30	$M_{23}C_6$	$\gamma_r + \sigma$	0.76	0.58
	60	$M_{23}C_6$	$\eta + \gamma_r + \sigma + \chi + R$	0.41	0.66
	120	$M_{23}C_6$	$\eta + \gamma_r + \sigma + \chi + R$	0.86	0.46
	240	$M_{23}C_6$	$\eta + \gamma_r + \sigma + \chi + R$	0.97	0.63
	600	$M_{23}C_6$	$\eta + \gamma_r + \sigma + \chi + R$	0.77	0.69

IV. DISCUSSION

The results of this study confirm the usefulness of the DL-EPR method in evaluating quantitatively the sensitization of austeno-ferritic DSS.[4,21,25–29] The DL-EPR method has the advantage of being a fast, quantitative, nondestructive test that can easily be incorporated into the monitoring of equipment exposed to localized corrosion risks in general and to IGC in particular. However, the sensitivity and the selectivity of the test in the detection of chromium-depleted zones seem to depend markedly on the type and temperature of the electrolyte and the potential scan conditions of the test.

Table VI. Chemical Composition (Weight Percent) of the Various Phases Present after Aging the UNS S31250 DSS

Phase	Cr	Ni	Mo	Si	Fe	Mn
$M_{23}C_6$	71.2	2.4	7.8	0.2	16.8	1.6
σ	35.8	2.7	8.7	0.8	50	2
χ	25	3	18.1	1.4	50	2.5
R	20	3.5	27	1.5	47.3	1
I	30	4.1	33.3	3	28.3	1.3
η	15	2.8	37	2.7	40.8	1.7

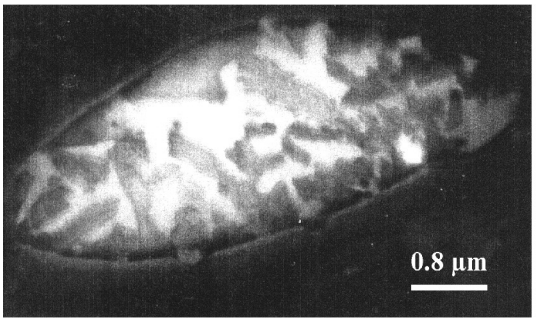

STEM image

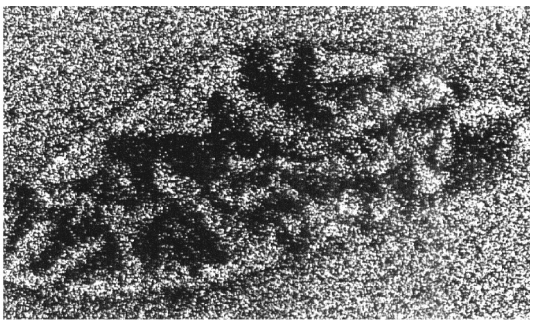

X-ray image, Cr Kα

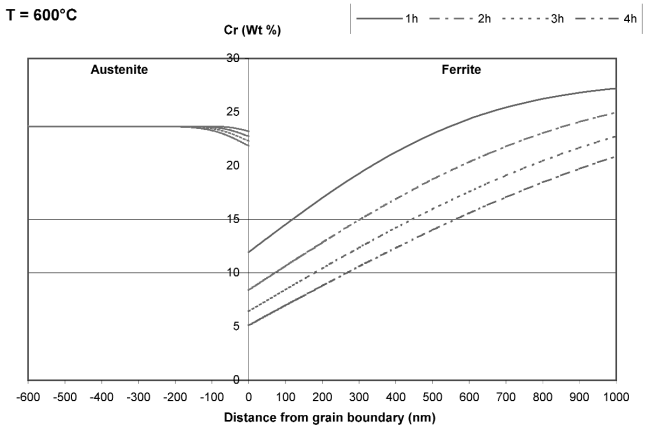

Fig. 15—Profiles of chromium depletion after aging at 600 °C.

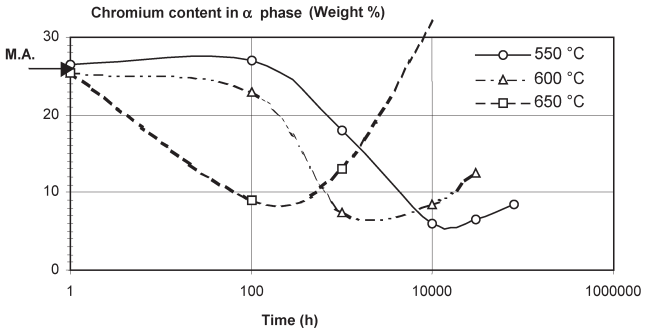

Fig. 16—Evolution of chromium content in the ferrite phase with different aging conditions, case of CF8M DSS[32] (MA: annealed material conditions).

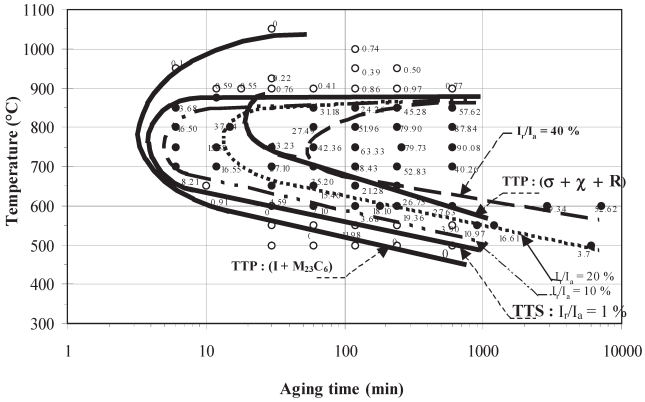

Fig. 17—TTP and TTS diagrams of UNS S31250 DSS from metallography and DL-EPR tests, respectively.

Activation and reactivation current densities depend significantly on the kind and the concentration of the depassivator, which, according to a model proposed by D. Reichert about the role of KSCN,[28] modifies the stability of the passive layer generated in an H_2SO_4 medium. In that model, the depassivator leads to the cracking of the passive layer during the anodic scan and to the dissolution of chromium-depleted zones, which have a less resistant passive film, during the reactivation scanning. For this reason, the anodic (I_a) and reactivation (I_r) current densities increase noticeably with depassivator concentration, in the case of KSCN[28] or KSCN + NaCl[4,21] or HCl (in Reference 19 and this study). In all cases, when the concentration reaches a threshold (0.02 M for KSCN and 0.3 pct of HCl), the ratio I_r/I_a stabilizes, the test selectivity decreases progressively, and a second reactivation peak appears at −290 mV/SCE. The latter corresponds to the apparition of high-density pitting in the initial austenite (Figures 5(b), 7(b), and 9(b)).

The choice of HCl as a depassivator seems to lead to the best test efficiency ($I_r/I_a \gg 1$ pct) and, in addition, to a good test selectivity, both in the case of super-austenitic SS[19] and in the case of the austeno-ferritic DSS considered in this study, compared to KSCN and NaCl, as illustrated by results reported in Table III. The use of HCl also guarantees high sensitivity with regard to lower-chromium-depleted zones. For example, the sensitization of steel type UNS S31250 aged over 1 hour at 600 °C was not detected by other electrolytes, such as Reicher's,

which consisted of H_2SO_4 + KSCN (I_r/I_a = 0.08 pct),[28] while this studied revealed a ratio I_r/I_a = 2.10 pct, using H_2SO_4 + HCl.

The optimum efficiency and optimum sensitivity of the H_2SO_4 + HCl electrolyte were obtained with a temperature of about 20 °C and a potential scanning rate of 2.5 mV/s. Higher temperatures (>20 °C) of the electrolyte and lower potential scan rates (<2.5 mV/s) may be more interesting, since these yield an increase of reactivation current I_r and improve the ratio I_r/I_a in general and especially in the case of low-sensitized materials. However, this advantage is quickly negated by the excessive exposure time in the electrolyte (imposed by the low scan rates) and by the high severity of the medium (induced by the decrease of the pH with temperature). These conditions modify noticeably the electrochemical reactivity of Duplex structures[34] and affect the DL-EPR test selectivity through the appearance of a second reactivation peak, at −290 mV/SCE, related to pitting or uniform corrosion.[28,35]

Microstructural investigations performed in this study reveal after DL-EPR tests a marked pitting in all austenitic grains, in agreement with the results of Roelandt and Vereecken[35] concerning the sensitized INCONEL 600* (73.5 pct Ni, 15.65 pct Cr).

*INCONEL is a trademark of INCO Alloys international, Huntington Woods, WV.

For this reason, most authors choose an electrolyte either at room temperature or near 30 °C[19,21,26] and potential scan rates between 0.5 and 5 mV/s, as shown in Table I.

The TTS diagram established from the DL-EPR test allows the determination of the field boundary of the IGC sensitization risk of UNS S31250 steel. It also offers the possibility of the quantitative evaluation of the degree of IGC sensitization. This qualifies the DL-EPR technique as an *in-situ* sensitization test of installations during service.[19] The superposition of TTS and TTP diagrams allows the elucidation of the interaction precipitation–IGC sensitization, during heating of UNS S31250 DSS. Four temperature ranges, characterizing these interactions, must be distinguished:

(a) At temperatures equal to or lower than 500 °C, the precipitation of the phase I (30 Cr wt pct) at α/γ interfaces leads to a weak chromium depletion, resulting on a low sensitization ($I_r/I_a \leq 15$ pct);
(b) Between 550 °C and 650 °C, nucleation of chromium carbides type $M_{23}C_6$ occurs at α/γ interfaces (Figure 3). These high-chromium carbides grow rapidly and chromium is removed from the ferritic phase, which initially has a higher chromium content. This leads to a significant chromium depletion and consequently to a high IGC sensitization ($I_r/I_a \leq 55$ pct). The results of the analytical calculation show the creation, at this temperature range, of a depleted zone near the α/γ interface and into the α phase. Chromium content can reach very low values (5 pct Cr), which leads to IGC sensitization and is revealed by the DL-EPR tests through the reactivation peak at −115 mV/SCE, with a density that grows higher as the chromium-depleted zone gets larger and the minimum chromium content gets lower.[33] This is in agreement with the IGC sensitization criteria indicated in References 32, 36, and 37: the chromium content is less than 13 pct and the profile width at this content is equal to or greater than 25 nm;
(c) Between 650 °C and 850 °C, the total eutectoid decomposition of ferrite into regenerate austenite (γ_r), carbides ($M_{23}C_6$) and intermetallic phases (χ, R, and σ), decreases the chromium content of interfaces, which show a higher IGC sensitization degree for longer periods of heating. This leads to ratios I_r/I_a reaching 90.08 pct after holding at 750 °C over 10 hours, in the case of the UNS S31250 DSS;
(d) At temperatures equal to or higher than 850 °C, sensitization is not detected ($I_r/I_a \leq 1$ pct) instead of the existence of precipitation phenomenon. At this temperature range, the rate of chromium carbide precipitation is relatively low, since the carbon solubility is higher in the austenite. In addition, the intermetallic phases are less stable, in this range of temperatures where the chromium diffusion rate is high, which ensures a fast rechromization of eventual chromium-depleted zones. Consequently, for those reasons, the absence of the formation of chromium-depleted zones explains the very low values of ratios ($I_r/I_a \leq 1$ pct). This result confirms the close relation between both the chromium depletion and IGC sensitization and the rechromization and the desensitization to the IGC.

V. CONCLUSIONS

The optimal conditions of the DL-EPR tests for evaluation of IGC sensitization of DSS adopted in this study are manifestly more efficient and more selective than the other existing conditions: they present the best ratio I_r/I_a for the high-sensitized steels and a high sensitivity in the detection of low sensitization. A reproducible DL-EPR test method was developed to characterize the degree of sensitization in DSS. This method makes use of a solution of 33 pct H_2SO_4 + 0.3 pct HCl at 20 °C, and a scan rate of 2.5 mV/s. The high selectivity and sensitivity of this test at a low degree of chromium depletion could lead to the future widespread use of this test as a fast, quantitative, and nondestructive technique for evaluating the IGC sensitization of DSS in cast pieces or wrought products.

The IGC sensitization of DSS is imputed to the chromium-depletion phenomenon resulting from the precipitation, at relatively low temperatures, of intermetallic phase I (Fe-Cr-Mo) and $M_{23}C_6$ carbides and the precipitation, at high temperatures, of $M_{23}C_6$ carbides and σphase (Fe-Cr-Mo). The contents of the other phases η, R, and χ are not enough to have a significant effect on chromium depletion.

The chromium-depletion phenomenon resulting from the precipitation of chromium carbides was analytically evaluated. The model used permitted the prediction of the chromium-depletion profiles corresponding to aging at 600 °C. These profiles show a significant chromium depletion in the ferritic phase. This is attributed to the fact that the chromium diffusion in the γ phase is 100 times lower than in the α phase.

It was shown also that the TTS diagram can be established with a high degree of accuracy by means of the DL-EPR test. In addition, the DL-EPR test enables the quantitative evaluation of the degree of the sensitization, which is useful in monitoring SS structures in service. The interactions

between precipitation and IGC sensitization during the aging of DSS have been well shown by the superposition of TTP and TTS diagrams.

REFERENCES

1. P. Combrade and J.P. Audouard: *Duplex Stainless Steels '91*, Proc. Conf., Beaune Bourgogne, France, 1991, J. Charles and S. Bernhardsson, eds., Les Editions de Physique, Paris, 1991, vol. 1, pp. 257-81.
2. J. Charles: *Duplex Stainless Steels '91*, Proc. Conf., Beaune Bourgogne, France, 1991, J. Charles and S. Bernhardsson, eds., Les Editions de Physique, Paris, 1991, vol. 1, pp. 151-68.
3. S. Azuma and K. Ogawa: *Appl. Thermal Eng*., 1998, vol. 18 (6), p. XXIV.
4. N. Lopez, M. Cid, M. Puiggali, I. Azkarate, and A. Pelayo: *Mater. Sci. Eng. A*, 1997, vol. 229 (1–2), pp. 123-28.
5. T. Amadou, A. Ben Rhouma, H. Sidhom, C. Braham, and J. Lédion: *Metall. Mater. Trans. A*, 2000, vol. 31A (8), pp. 2015-24.
6. B. Josefsson, J.O. Nilsson, and A. Wilson: *Duplex Stainless Steels '91*, Proc. Conf., Beaune Bourgogne, France, 1991, J. Charles and S. Bernhardsson, eds., Les Editions de Physique, Paris, 1991, vol. 1, pp. 67-78.
7. M. Guttmann: *Duplex Stainless Steels '91*, Proc. Conf., Beaune Bourgogne, France, 1991, J. Charles and S. Bernhardsson, eds., Les Editions de Physique, Paris, 1991, vol. 1, pp. 79-92.
8. Report No. NF EN ISO 3651-2, AFNOR, Cedex, France, 1998.
9. NF EN ISO 3651-1, AFNOR, Cedex, France, 1998.
10. *Practice A262-98, Standard Practices for Detecting Susceptibility to Intergranular Attack in Austenitic Stainless Steels*, ASTM, New York, NY, 1998.
11. *Test Method G28-97, Standard Test Methods of Detecting Susceptibility to Intergranular Corrosion in Wrought, Nickel-Rich, Chromium-Bearing Alloys*, ASTM, New York, NY, 1997.
12. V. Cihal, A. Desestret, M. Froment, and G.-H. Wagner: *5th Eur. Conf. on Corrosion*, Proc. Conf., Paris, 1973, pp. 249-54.
13. T. Wu, T. Cheng and W. Tsai: *J. Nucl. Mater*., 2001, vol. 295 (2–3), pp. 233-43.
14. V. Cíhal and R. Ctefec: *Electrochimica Acta*, 2001, vol. 46 (24–25), pp. 3867-77.
15. M. Verneau, C. Lojewski, and J. Charles: *Duplex Stainless Steels '91*, Proc. Conf., Beaune Bourgogne, France, 1991, J. Charles and S. Bernhardsson, eds., Les Editions de Physique, Paris, 1991, vol. 2, pp. 863-70.
16. M. Verneau, F. Dupoiron, and J. Charles: *12th Int. Corrosion Conf*., Proc. Conf., Houston, TX, 1993.
17. M. Verneau and J.M. Scarabello: *Corrosion in Chemical and Parachemical Industries*, 2nd Eur. Conf. on corrosion, Proc. Conf., Grenoble, France, 1994, CEFRACOR, Paris, France, 1994, pp. 181-82.
18. I. Chattoraj, A.K. Bhattamishra, S. Jana, S.K. Das, S.P. Chakraborty, and P.K. De: *Corr. Sci*., 1996, vol. 38 (6), pp. 957-69.
19. Y. Cetre, P. Eichner, G. Sibaud, and J.M. Scarabello: *Corrosion in Chemical and Parachemical Industries* 3rd Eur. Conf. on Corrosion, Proc. Conf., Lyon, France, 1997, CEFRACOR, Paris, France, 1997, pp. C4.1-C4.12.
20. M. Verneau, J. Charles, and C. Lojewski: *Corrosion in Chemical and Parachemical Industries*, 1st Eur. Conf. on corrosion, Proc. Conf., Lyon, France, 1991, CEFRACOR, Paris, France, 1991, pp. P17.1-P17.6.
21. N. Lopez: Ph.D. Thesis, University of Bordeaux I, Bordeaux, France, 1997.
22. F. Mazaudier, G. Sanchez, and P. Fauvet: *Corrosion in Chemical and Parachemical Industries*, 3rd Eur. Conf. on Corrosion, Proc. Conf., Lyon, France, 1997, CEFRACOR, Paris, France, 1997, pp. 12.1-12.6.
23. A.P. Majidi and M.A. Streicher: *Corr. Nace*, 1984, vol. 40 (8), pp. 393-408.
24. A.P. Majidi and M.A. Streicher: *Corr. Nace*, 1984, vol. 40 (11), pp. 584-93.
25. M. Verneau and B. Bonnefois: *Corrosion in Chemical and Parachemical Industries*, 3rd Eur. Conf. on Corrosion, Proc. Conf., Lyon, France, 1997, CEFRACOR, Paris, France, 1997, C5.1-C5.6.
26. U. Kamachi Mudali, R.K. Dayal, J.B. Gnanamoorthy, and P. Rodriguez: *Metall. Mater. Trans. A*, 1996, vol. 27A, pp. 2881-87.
27. S.J. Goodwin, B. Quayle, and F.W. Noble: *Corr. Nace*, 1987, vol. 43 (12), pp. 743-47.
28. David L. Reichert and Glenn E. Stoner: *Electrochem Soc*., 1990, vol. 137 (2), pp. 411-13.
29. J.R. Scully and R.G. Kelly: *Corr. Nace*, 1986, vol. 42 (9), pp. 537-42.
30. H. Sidhom and R. Portier: *Phil. Mag. Lett*., 1989, vol. 59 (3), pp. 131-39.
31. H. Sidhom, S. Bonnet, and R. Portier: *3rd Int. Meeting on Quasicrystals and Incommensurate Structures*, Proc. Conf., Vista Hermosa, Mexico, 1989, M. Morelos, ed., World Scientific Pub. Co., New York, 1990.
32. H. Sahlaoui, H. Sidhom, and J. Philibert: *Acta Mater*., 2002, vol. 50 (6), pp. 1383-92.
33. H. Sidhom: Ph.D. Thesis, University of Paris XI, Paris, 1990.
34. I. Trigui, H. Sidhom, C. Braham, and J. Lédion: *Mater. Technol*., 1996, June, pp. 23-30.
35. A. Roelandt and J. Vereecken: *Corr. Nace*, 1986, vol. 42 (5), pp. 289-98.
36. C. Stawström and M. Hillert: *J. Iron Steel Inst*., 1969, Jan., pp. 77-85.
37. A. Borello and S. Casadio: *Corr. Nace*, 1981, vol. 37 (9), pp. 498-505.